Equilibrium Folding of Dimeric Class μ Glutathione Transferases Involves a Stable Monomeric Intermediate[†]

Judith A. T. Hornby,[‡] Jiann-Kae Luo,[‡] Julie M. Stevens,[‡] Louise A. Wallace,[‡] Warren Kaplan,[‡] Richard N. Armstrong,[§] and Heini W. Dirr*,[‡]

Protein Structure−Function Research Program, Department of Molecular and Cell Biology, University of the Witwatersrand, Johannesburg 2050, South Africa, and Department of Biochemistry and Center in Molecular Toxicology, Vanderbilt University School of Medicine, Nashville, Tennessee 37232

Received January 31, 2000; Revised Manuscript Received May 10, 2000

ABSTRACT: The conformational stabilities of two homodimeric class μ glutathione transferases (GSTM1-1 and GSTM2-2) were studied by urea- and guanidinium chloride-induced denaturation. Unfolding is reversible and structural changes were followed with far-ultraviolet circular dichroism, tryptophan fluorescence, enzyme activity, chemical cross-linking, and size-exclusion chromatography. Disruption of secondary structure occurs as a monophasic transition and is independent of protein concentration. Changes in tertiary structure occur as two transitions; the first is protein concentration dependent, while the second is weakly dependent (GSTM1-1) or independent (GSTM2-2). The second transition corresponds with the secondary structure transition. Loss in catalytic activity occurs as two transitions for GSTM1-1 and as one transition for GSTM2-2. These transitions are dependent upon protein concentration. The first deactivation transition coincides with the first tertiary structure transition. Dimer dissociation occurs prior to disruption of secondary structure. The data suggest that the equilibrium unfolding/refolding of the class μ glutathione transferases M1-1 and M2-2 proceed via a three-state process: $N_2 \leftrightarrow 2I \leftrightarrow 2U$. Although GSTM1-1 and GSTM2-2 are homologous (78% identity/94% homology), their N_2 tertiary structures are not identical. Dissociation of the GSTM1-1 dimer to structured monomers (I) occurs at lower denaturant concentrations than for GSTM2-2. The monomeric intermediate for GSTM1-1 is, however, more stable than the intermediate for GSTM2-2. The intermediates are catalytically inactive and display nativelike secondary structure. Guanidinium chloride-induced denaturation yields monomeric intermediates, which have a more loosely packed tertiary structure displaying enhanced solvent exposure of its tryptophans and enhanced ANS binding. The three-state model for the class μ enzymes is in contrast to the equilibrium two-state models previously proposed for representatives of classes α/π/Sj26 GSTs. Class μ subunits appear to be intrinsically more stable than those of the other GST classes.

Previous work on protein folding has concentrated on small proteins that fold rapidly and avoid aggregation. However, most protein chains are more than 100 residues long and have been shown to fold via intermediate states that are populated enough to be detectable. The folding of multimeric proteins involves not only the intramolecular interactions as a polypeptide chain associates with itself but also the intermolecular interactions as it associates with other monomers. Thus, issues of additional stability conferred to oligomeric proteins by means of their intermolecular interactions at the subunit interface can only be addressed in oligomeric proteins. Studies revealing the properties important for the formation and stabilization of these oligomeric proteins include such systems as the Arc repressor (*1*), the GCN4 leucine zipper peptide (*2*), legume lectins (*3*), BDNF (*4*), CRP (*5*), and the Trp repressor (*6*).

A protein's folding mechanism, three-dimensional structure, and conformational stability are determined by its unique amino acid sequence (*7*). Defining the complete folding pathway involves identifying and characterizing all conformational states (stable and transient) that exist along the folding and unfolding pathways.

To establish the thermodynamic requirements for and the involvement of the quaternary structure in subunit stability/folding/assembly of the cytosolic glutathione transferases (EC 2.5.1.18, GSTs),[1] we studied the conformational stabilities of two mammalian homodimeric class μ GST isozymes (GSTM1-1 and GSTM2-2). They are members of a super-

[†] This work was supported by the University of the Witwatersrand, the South African National Research Foundation, the Fogarty International Collaboration Award TW00779, Grant GM30910 from the National Institutes of Health, and the Alexander von Humboldt Foundation.

* To whom correspondence should be addressed: e-mail 089dirr@cosmos.wits.ac.za; fax +27 11 403 1733; phone +27 11 716 2265.

[‡] University of the Witwatersrand.

[§] Vanderbilt University School of Medicine.

[1] Abbreviations: GST, glutathione transferase; GSTM1-1, GSTM2-2, GSTA1-1, and GSTP1-1, glutathione transferases from classes μ, α and π, respectively, with two type 1 or type 2 subunits; sj26GST, glutathione transferase from *Schistosoma japonicum*; ANS, anilinonaphthalene sulfonate; EDTA, ethylenediaminetetraacetic acid; SEC−HPLC, size-exclusion high-performance liquid chromatography; Gdm-Cl, guanidinium chloride.

10.1021/bi000176d CCC: $19.00
Published on Web 09/13/2000

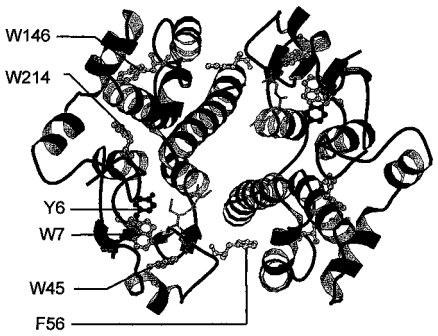

FIGURE 1: Ribbon representation of class μ rGSTM1-1 (*20*) viewed down the 2-fold axis. The active-site ligand glutathione is represented in stick form and the Tyr6, Phe56, Trp7, Trp 45, Trp 146, and Trp214 residues are shown as ball-and-stick models. Phe56 represents the location of the hydrophobic lock-and-key interaction.

gene family of multifunctional proteins that play a central role in the detoxification of xenobiotics. Enzymes of this family of dimeric proteins can be grouped into a variety of species-independent gene classes (see ref *8*) and many high-resolution crystal structures of representatives of all the cytosolic GST classes have been elucidated, making this superfamily an ideal model for the study of dimeric protein folding, stability, and assembly. Dimerization is highly specific and occurs only between subunits within the same gene class, resulting in the formation of homo- and heterodimers. Crystal structures for the family display a highly conserved, archetypical fold (see review in ref *9*), as illustrated in Figure 1 for GSTM1-1. The GSTM1/M2 polypeptide has 217 amino acids that fold into two structural domains (a smaller α/β domain I and an all-α domain II) with no disulfide bonds. The tertiary fold of domain I of each GST monomer has been identified through X-ray crystallography as the glutathione binding site in a number of monomeric proteins such as thioredoxins (*10*), glutathione peroxidases (*11*), glutathione reductases (*12*), and thiotransferases (*13*). The principal intersubunit interactions occur between domain I of one subunit and domain II of the other subunit. Structural features at the dimer interfaces of the GSTs suggest two major groupings of subunit interfaces, the $\alpha/\mu/\pi$/Sj26 subunit type and the σ/θ subunit type (*8*). The interface for the former group is curved, hydrophobic, and involves a prominent hydrophobic lock-and-key intersubunit interaction motif (see Figure 1), whereas the interface for the latter group is flatter, more hydrophilic, and lacks the lock-and-key motif.

GSTs are stable homo- or heterodimers ($M_r \sim 50\,000$) with no spontaneous exchange of subunits occurring between enzyme molecules. Why are GSTs dimeric? Answers lie in both protein function and stability. The dimeric structure is important for the formation of fully functional catalytic sites near the subunit interface in classes $\alpha/\mu/\pi$/Sj26/σ [but not in class θ (*14*)], as well as in the formation of a non-substrate−ligand binding region in the amphipathic cleft at the dimer interface (*15*−*17*). To date, equilibrium unfolding studies with representatives of the α/π/Sj26 subunit grouping [i.e., hGSTA1-1 (*18*), pGSTP1-1 (*19, 20*), and Sj26GST (*21*)] indicate that there exists a tight coupling in these proteins between dissociation/association and unfolding/refolding. No stable intermediates were detected and the size of the protein was found to be the major structural determinant for conformational stability. These findings suggest that the dimeric quaternary structure is essential for stabilizing the tertiary structures of the individual subunits within this grouping of GSTs. The nature of the dimer interface can, however, impact on GST conformational stability and folding as shown in a study with class σ GSTS1−1 (*22*) that exhibits stable dimeric and monomeric folding intermediates.

In the present study, solvent-induced unfolding of class μ GSTs was followed under equilibrium conditions by monitoring enzyme activity and ANS binding (functional probes), and far-ultraviolet circular dichroism, tryptophan fluorescence, chemical cross-linking, and size-exclusion chromatography (secondary, tertiary and quaternary structure probes). The unfolding transitions, their protein concentration dependent behavior, and the cross-linking and size-exclusion chromatography data support a three-state equilibrium folding model for class μ GSTs involving a stable monomeric intermediate. This is clearly in contrast to the two-state models reported for their homologues in classes α/π/Sj26 GSTs.

EXPERIMENTAL PROCEDURES

Materials. Rat GSTM1-1 and GSTM2-2 were overexpressed in *Escherichia coli* M5219 strain transformed with the plasmids pGT33MX and pGT44, respectively, according to ref *23*. The ligand-free enzymes were purified by cation-exchange chromatography on CM-Sephadex in 20 mM sodium phosphate buffer, pH 7.0, during which the protein eluted at 150 mM NaCl. Protein was stored in 20 mM sodium phosphate buffer, pH 6.5, with 0.1 M NaCl and 0.02% sodium azide. The concentration of the protein dimers was determined at 280 nm using an extinction coefficient of 81 480 M^{-1} cm^{-1} (*24*). Ultrapure urea and GdmCl were purchased from ICN and Boehringer, respectively. All other chemicals were of analytical grade.

Unfolding Studies. Equilibrium unfolding and reversibility experiments were carried out at 25 °C in 20 mM sodium phosphate, 100 mM NaCl, and 1 mM EDTA buffer, pH 6.5, according to the methods described for other GSTs (*18*−*22*). Conditions for enzyme assays yielded linear progress curves with less than 10% reactivation for the unfolded enzyme occurring during the assays. Tryptophan fluorescence (excitation at 295 nm) was measured at 335 and 355 nm for folded and unfolded protein, respectively. Rayleigh scattering measurements at 295 nm (emission and excitation) indicated the absence of aggregation during the unfolding/refolding processes. Far-ultraviolet (200−250 nm) circular dichroism data were obtained in a Jasco J-710 spectropolarimeter with a 1 mm path length as described (*22*). Protein cross-linking experiments with glutaraldehyde were performed as described (*29*) and run on SDS−15% PAGE. Tryptophan fluorescence quenching with acrylamide was performed as described (*19*).

Data Analysis. Analyses of the unfolding transitions and determination of conformational stability parameters (i.e., C_m, transition midpoint; ΔG, free energy change; m value, dependence of free energy on denaturant concentration) were performed according to either a two-state model (*25*)

$$N_2 \leftrightarrow 2U$$

or a three-state model (*26*−*28*)

$$N_2 \overset{K_1}{\longleftrightarrow} 2I \overset{K_2}{\longleftrightarrow} 2U$$

where N_2 is the native dimer, I is a monomeric intermediate, U is the unfolded polypeptide and K_1 and K_2 are the equilibrium constants for the dissociation/association and unfolding/refolding steps, respectively. Free energy changes (ΔG_1 and ΔG_2) are derived from the K_1 and K_2 equilibrium constants:

$$\Delta G_1 = -RT \ln K_1 \quad \text{and} \quad \Delta G_2 = -RT \ln K_2$$

where R is the gas constant and T is the absolute temperature. The change in free energy is assumed to be a linear function of denaturant concentration (see ref *28*):

$$\Delta G_1 = \Delta G_1(H_2O) - m_1[\text{denaturant}]$$

and

$$\Delta G_2 = \Delta G_2(H_2O) - m_2[\text{denaturant}]$$

where $\Delta G(H_2O)$ is the free energy change in the absence of denaturant.

When using spectroscopy techniques to monitor the unfolding of a protein via the three-state unfolding model above, the global signal (Y) may be expressed as:

$$Y = Y_n + \{([(Y_I - Y_n)/(Y_u - Y_n)]I + U)/2C\}(Y_u - Y_n)$$

where Y_n, Y_i, Y_u, and Y_d are the molar signals (M^{-1}) for states N_2, I, U, and the denaturant, respectively. Y_n and Y_u are assumed to be linear functions of denaturant concentration, while Y_i is a constant since the intermediate only exists over a narrow range of denaturant concentration. C is the total protein monomer concentration, and U and I are the fractions of unfolded and intermediate protein at equilibrium, respectively (O. Bilsel, personal communication). Equations for solving for the U, I, and N_2 species at equilibrium are

$$U = 0.25K_1K_2\{(1 + K_2) + \sqrt{[(1 + K_2)^2 + 16C/K_1]}\}$$

$$I = U/K_2$$

$$N_2 = I_2/K_1$$

All equilibrium unfolding data were fitted by nonlinear least-squares with the Jandel Scientific software SigmaPlot ver 5.00.

RESULTS

Structural and Functional Probes. In light of the structural complexity of GSTM1-1 and GSTM2-2, a variety of structural and functional probes were used to monitor changes occurring at different structural levels during the unfolding/refolding processes. Far-ultraviolet circular dichroism monitored the disruption of secondary structure, while perturbations in tertiary and quaternary structure were monitored by enzymatic activity [which should be sensitive to changes at or near the dimer interface due to the contribution of Asp105 from a neighboring subunit toward the active site (*30*)]. Tryptophan fluorescence (there are four tryptophans per subunit, at positions 7 and 45 in domain I and at 146 and 214 in domain II) and the binding of the nonsubstrate ligand ANS to the amphipathic groove at the dimer interface (*15*) were also used to monitor the tertiary and quaternary structural changes in the proteins. Chemical cross-linking/SDS−PAGE and SEC−HPLC monitored the appearance of monomeric species and changes in the hydrodynamic volume.

According to its crystal structure (*30*), about 74% of the amino acids in GSTM1-1 are involved in secondary structure (49% in α-helices, 10% as β-strands, 15% as β-turns). The far-ultraviolet circular dichroism spectra obtained for GSTM1-1 and GSTM2-2 are similar [Figures 2A (inset) and 4A (inset), respectively] with peaks of negative ellipticity at 210 and 220 nm consistent with its high α-helical content. Secondary structure is completely disrupted as the proteins unfold; there is no significant ellipticity at >220 nm in the presence of 8.4 M urea, indicating that the unfolded polypeptides assume a random coil conformation. Although both have the same number of tryptophan residues, there is spectroscopic evidence that the tertiary environments of the tryptophans are different. Fluorescence spectra of folded and unfolded class μ GSTs [Figures 3A (inset) and 5A (inset)] indicate complete exposure of the buried tryptophans to solvent during unfolding (red shift in emission maximum from 335 to 355 nm). This red shift was accompanied by enhanced emission intensity (~1.7-fold for GSTM1-1 and ~1.1-fold for GSTM2-2). The fluorescence intensity at 335 nm of folded GSTM1-1 is about 42% lower than that observed for GSTM2-2, suggesting differences in the microenvironments of the tryptophan residues in the two proteins. According to the crystal structure of rGSTM1-1 (*30*) and the homology model built with Whatif (*31*) for GSTM2-2 (no crystal structure is available for rGSTM2-2), the tryptophans of GSTM1-1 appear to be in a more quenching chemical environment than those of GSTM2-2 (i.e., the side chains of several charged residues in rGSTM1-1 are in close proximity to the four tryptophans and are thus capable of quenching their fluorescence in the folded protein). The environments in the unfolded proteins are similar as indicated by the similar fluorescence spectra for unfolded GSTM1 and GSTM2.

The accessibility of the tryptophans in native GSTM1-1 and GSTM2-2 to solvent was determined by the ability of acrylamide to quench tryptophan fluorescence. Stern−Volmer plots were linear with no upward curvature, indicating that quenching occurs predominantly via a dynamic collisional mechanism. Stern−Volmer quenching constants (K_{SV}) of 4.7 M^{-1} and 9.3 M^{-1} for GSTM1-1 and GSTM2-2, respectively, are indicative of a greater solvent exposure for the tryptophans in GSTM2-2. Fluorescence anisotropy data obtained for folded and unfolded GSTM1-1 (0.073 and 0.03, respectively) and for GSTM2-2 (0.070 and 0.039, respectively) suggest that the hydrodynamic volumes for the folded and unfolded states are similar to those observed for other GSTs (*20*, *22*).

Equilibrium Unfolding of GSTM1-1 and GSTM2-2. The reversibility of urea- and GdmCl-induced unfolding of class μ GSTs was estimated to be 100% and >70% for fluorescence and enzyme activity, respectively, indicating that the refolded enzymes were structurally and functionally similar to the native proteins. Unfolding curves for GSTM1-1 are shown in Figures 2 and 3 for urea and GdmCl, respectively, while the curves for GSTM2-2 are shown in Figures 4 and 5 for urea and GdmCl, respectively. The protein concentra-

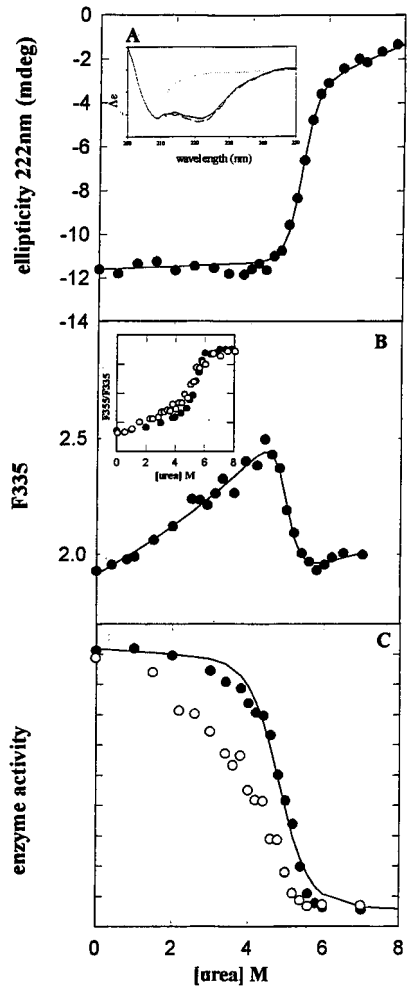

FIGURE 2: Urea-induced unfolding transitions for 2 μM rGSTM1-1 were monitored by (A) ellipticity at 222 nm, and far-UV CD spectra in the presence of no urea (—), 4.2 M urea (- - -), and 8 M urea (•••) (inset); (B) tryptophan fluorescence [excitation at 295 nm and emission measured at 335 nm (folded protein)]; and (C) loss of enzyme activity. The protein concentration dependence of the tryptophan fluorescence [excitation at 295 nm and emission measured at 335 nm (folded protein) and 355 nm (unfolded protein) (inset to B)] and enzyme activity unfolding transitions were determined at 0.2 μM (○) and 2 μM (●). The solid lines represent fits to the data from which the thermodynamic parameters were obtained (see Table 1). Conditions were 20 mM sodium phosphate, 0.1 M NaCl, and 1 mM EDTA, pH 6.5.

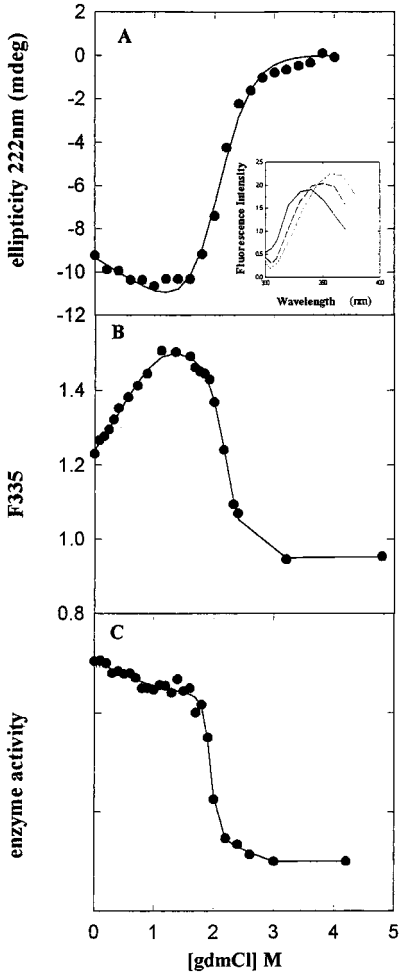

FIGURE 3: GdmCl-induced unfolding transitions for 2 μM GSTM1-1 were monitored by (A) ellipticity at 222 nm; (B) tryptophan fluorescence [excitation at 295 nm and emission measured at 335 nm (folded protein)]; and (C) loss of enzyme activity. The fluorescence spectra of the representative states, native (—), intermediate (- - -), and unfolded (•••) are presented in the inset. The solid lines represent fits to the data from which thermodynamic parameters were determined (see Table 1). Conditions were as described for Figure 2.

tion dependent behavior of the unfolding transitions was determined at 0.2 μM (○) and 2 μM (●) in order to differentiate between unimolecular (concentration-independent) and bimolecular (concentration-dependent) steps. Disruption of secondary structure, as measured by ellipticity at 222 nm (Figures 2−4), occurs as a monophasic sigmoidal transition and was independent of protein concentration between 0.5 and 2 μM (lower concentrations yielded poor signals). Changes in tertiary structure, as monitored by tryptophan fluorescence, are biphasic, indicating that the unfolding mechanisms for the class μ isoenzymes are not simple two-state processes. The first phase occurs at lower denaturant and is dependent on protein concentration, while the second phase at higher denaturant activity is weakly dependent (GSTM1-1) or independent (GSTM2-2). The second phase corresponds with the second structure transition. At low denaturant concentrations, the fluorescence properties of GSTM1-1 display a greater dependence on denaturant than those observed for GSTM2-2. At low concentrations, GdmCl has a greater impact on the emission maximum wavelength of tryptophan fluorescence than does urea. A larger red shift of 8−9 nm occurs during the first fluorescence phase (0−1.8 M GdmCl) of both proteins, indicating that the tryptophans become more exposed to solvent with GdmCl than with urea during this phase. Loss in catalytic activity is biphasic for GSTM1-1 and is monophasic for GSTM2-2. The first inactivation phase for GSTM1-1 and the inactivation transition for GSTM2-2 are dependent upon protein concentration. The first inactivation phase corresponds with the first tertiary structure (fluorescence) phase. Table 1 summarizes the parameters for the equilibrium unfolding of GSTM1-1 and GSTM2-2.

ANS Binding. Although folded proteins in general do not bind ANS, native cytosolic GSTs bind ANS. Binding of the amphipathic dye occurs at the dimer interface (*15*, *22*) and has little impact on GST conformational stability (*20*). When ANS binds the class μ enzymes (K_d of 77 μM), its emission maximum decreases from 535 nm to 490−500 nm, ac-

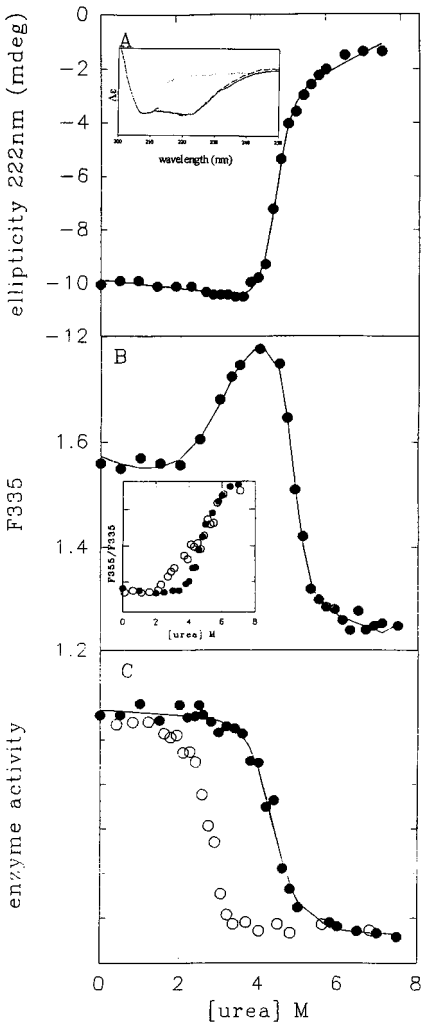

FIGURE 4: Urea-induced unfolding transitions for 2 μM GSTM2-2 were monitored by (A) ellipticity at 222 nm and far UV CD spectra in the presence of no urea (—), 4.0 M urea (- - -), and 8 M urea (•••) (inset); (B) tryptophan fluorescence [excitation at 295 nm and emission measured at 335 nm (folded protein)]; and (C) loss of enzyme activity. The protein concentration dependence of the tryptophan fluorescence [excitation at 295 nm and emission measured at 335 nm (folded protein) and 355 nm (unfolded protein) (inset to B)] and enzyme activity unfolding transitions were determined at 0.2 μM (○) and 2 μM (●). The solid lines represent fits to the data from which thermodynamic parameters were determined (see Table 1). Conditions were as described for Figure 2.

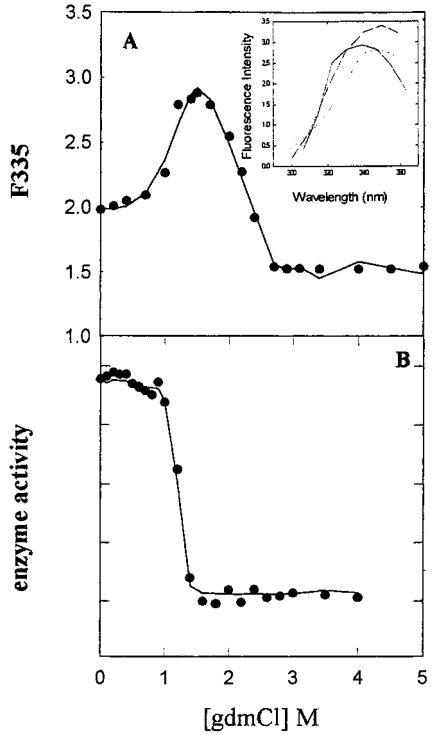

FIGURE 5: GdmCl-induced unfolding transitions for 2 μM GSTM2-2 were monitored by (A) tryptophan fluorescence [excitation at 295 nm and emission measured at 335 nm (folded protein)] and (B) loss of enzyme activity. The fluorescence spectra of the representative states, native (—), intermediate (- - -), and unfolded (•••), are presented in the inset. The solid lines represent fits to the data from which thermodynamic parameters were determined (see Table 1). Conditions were as described for Figure 2.

companied by enhanced fluorescence intensity. The spectral blue shift demonstrates that the environment of the ANS binding site is hydrophobic. However, the class μ site is not as apolar as the site in hGSTA1-1, pGSTP1-1, GSTS1-1, and Sj26GST, all of which display a much larger Stokes blue shift for the bound dye's emission maximum (*15*, *20*, *22*; Sayed and Dirr, unpublished results). Unfolded GST does not bind ANS. In addition to using ANS to probe the ligandin site at the dimer interface, the dye can also be used to monitor the extent of packing of hydrophobic cores in proteins undergoing structural changes (*32*). The effect of denaturant on the ability of GSTM1-1/GSTM2-2 to bind ANS is shown in Figure 6. When urea is used as denaturant, ANS binding follows a trend similar to that seen with tryptophan fluorescence and enzyme activity (see Figures 3 and 5), while with GdmCl as denaturant, there is enhanced ANS binding corresponding with the first tryptophan fluorescence phase and enzyme activity transition observed at 0−1.8 M GdmCl (see Figures 4 and 6). Global unfolding at higher denaturant concentrations results in a complete loss of ANS binding.

Chemical Cross-Linking and SEC−HPLC. Chemical cross-linking experiments with glutaraldehyde indicate that monomeric species begin to appear at about 2 M urea/0.5 M GdmCl for GSTM1-1 (Figure 7A) and at about 3.5 M urea/1 M GdmCl for GSTM2-2 (Figure 7B). In SEC−HPLC experiments under conditions similar to those used for spectroscopic/function data collection, single physical states corresponding to native dimeric, monomeric, and unfolded monomeric protein were observed at low and high urea concentrations, respectively (Figure 8). The elution volumes for the folded and unfolded μ GSTs are similar to those obtained for other GSTs (see ref *21*).

Thermal Denaturation. GSTM1-1 has a higher thermal stability than GSTM2-2 as reflected in their melting temperatures determined by circular dichroism at 222 nm; T_m values are 60 °C for M1-1 and 54 °C for M2-2 (Figure 9). Melting curve slopes were similar for both enzymes. GSTM1-1's higher T_m values are consistent with its higher ΔG values obtained with urea and GdmCl (Table 1). Unlike solvent-induced denaturation, thermal denaturation is irreversible due to protein aggregation at high temperatures, making the protein unsuitable for calorimetric studies.

DISCUSSION

The overall unfolding pathway for the homodimeric proteins GSTM1-1 and GSTM2-2 must begin with folded

Table 1: Thermodynamic Parameters for Urea and GdmCl Equilibrium Denaturation of 2 μM rGSTM1-1 and rGSTM2-2[a]

	m_1 [kcal/(mol·M)]	m_2 [kcal/(mol·M)]	$\Delta G(H_2O)^1$ (kcal/mol)	$\Delta G(H_2O)^2$ (kcal/mol)	C_{m1} (M)	C_{m2} (M)
			Urea			
M1-1						
CD[b]		3.38 ± 0.02		19.60 ± 0.21		5.3
act.[b]	2.12 ± 0.26		14.04 ± 1.2		4.8	
fl[c]	0.98 ± 0.2	3.45 ± 0.30	10.81 ± 1.8	16.50 ± 0.13	3.1	5.2
M2-2						
CD[b]		3.67 ± 0.25		17.1 ± 1.0		4.8
act.[b]	2.31 ± 0.21		12.74 ± 0.7		4.1	
fl[c]	1.82 ± 0.10	3.11 ± 1.09	12.40 ± 0.9	14.81 ± 0.75	3.2	5.0
			GdmCl			
M1-1						
CD[b]		4.80 ± 0.30		17.0 ± 1.22		2.2
act.[c]	1.12 ± 0.21	6.32 ± 0.25	8.96 ± 0.52	11.80 ± 1.92	1.5	2.3
fl[c]	2.20 ± 0.2	5.11 ± 0.52	9.15 ± 0.85	16.31 ± 3.51	1.8	2.4
M2-2						
act.[b]	3.82 ± 0.05		10.22 ± 0.78		1.3	
fl[c]	3.33 ± 0.034	6.05 ± 0.58	9.80 ± 0.58	15.81 ± 1.084	1.1	2.4

[a] Measurements were made at 25 °C, pH 7.0. Regression coefficients of the individual fits were all greater than 0.967 and the residuals show less than 5% deviation. [b] Fitted according to the two-state model (*15*). [c] Fitted according to the three-state model ($N_2 \leftrightarrow 2I \leftrightarrow 2U$) (*16*−*18*).

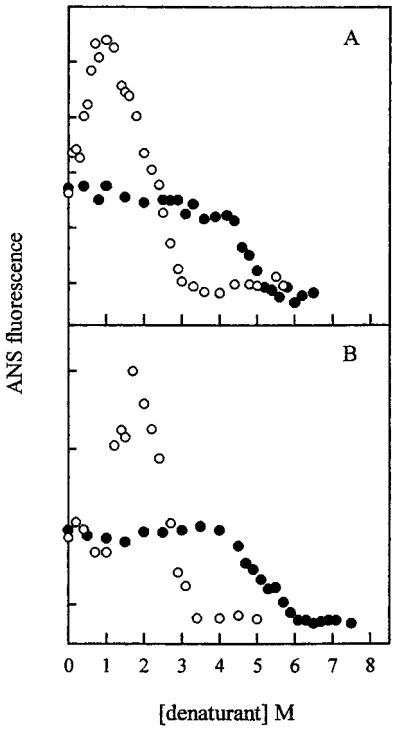

FIGURE 6: Effect of urea (●) and GdmCl (○) on the binding of ANS to 2 μM GSTM1-1 (A) and GSTM2-2 (B). The binding of the ligand ANS was monitored by direct excitation (400 nm) and emission at 490 nm (arbitrary units) following the addition of 200 μM ANS to the protein samples at 25 °C, pH 6.5.

dimer (N_2) and end with two unfolded monomers (2U). The way in which this can be achieved depends on whether intermediates are present along the pathway; e.g., $N_2 \leftrightarrow 2U$ for a two-state model and $N_2 \leftrightarrow 2N$ (or 2I or I_2) $\leftrightarrow 2U$, for a three-state model, where N is native monomer, I is a monomeric intermediate, and I_2 is a dimeric intermediate. The two-state model is a concerted and bimolecular dissociation/unfolding process for which one expects monophasic unfolding curves, superimposable for all spectroscopic probes used to monitor unfolding at a fixed denaturant concentration. The transitions observed with this model should be protein concentration dependent. For the three-state models, biphasic curves and/or noncoincident unfolding transitions are expected if the probes used can distinguish between the different conformational states. Protein concentration dependent behavior can also be used to differentiate between the three-state models (i.e., 2N and 2I vs I_2), in that only the bimolecular steps should be protein concentration dependent. If the first transition is bimolecular, subunit dissociation is occurring and the intermediate is a monomer. If however, it is the second transition that is protein concentration dependent, then subunit dissociation occurs after the formation of a dimeric intermediate.

The data from this study suggest an unfolding model involving an initial protein concentration dependent (bimolecular) step followed by a protein concentration independent (unimolecular) step. Enzyme activity appeared to be most sensitive toward the bimolecular step, whereas far-UV circular dichroism was sensitive only toward the unimolecular step. ANS binding and tryptophan fluorescence were sensitive to both. Therefore, dimer dissociation occurs prior to the disruption of secondary structure and the equilibrium unfolding/refolding of GSTM1-1 and GSTM2-2 most likely proceeds via a three-state process: $N_2 \leftrightarrow 2I \leftrightarrow 2U$. This multistate unfolding/refolding model for the class μ GST enzymes is in contrast to the highly cooperative and concerted two-state models that have been proposed for class α/π/Sj26 GSTs (*18*−*21*). The sum of the *m* values (m_1 and m_2) for certain probes listed in Table 1 is in reasonable agreement with the surface area predicted to become exposed upon unfolding; values calculated according to ref *33* are 4.7 $kcal^{-1}$ mol (M urea)$^{-1}$ and 9.5 $kcal^{-1}$ mol (M GdmCl)$^{-1}$ for both class μ GSTs. The smaller values for m_1 are consistent with the dissociation of the dimer to two structured monomers, while the larger m_2 values for the unfolding of the monomers would be expected due to a greater exposure of surface area. Inspection of the X-ray structure of the folded native dimeric protein provides support for this observation. The populational distribution of the native, intermediate, and unfolded forms of the proteins is shown in Figure 10. According to this model, the GSTM1-1 intermediate appears at 0.1 M urea and predominates at 4.2 M urea, while the GSTM2-2 intermediate only appears at 1.4 M urea. The unfolded forms do not appear until 4.4 and 4.3 M urea for

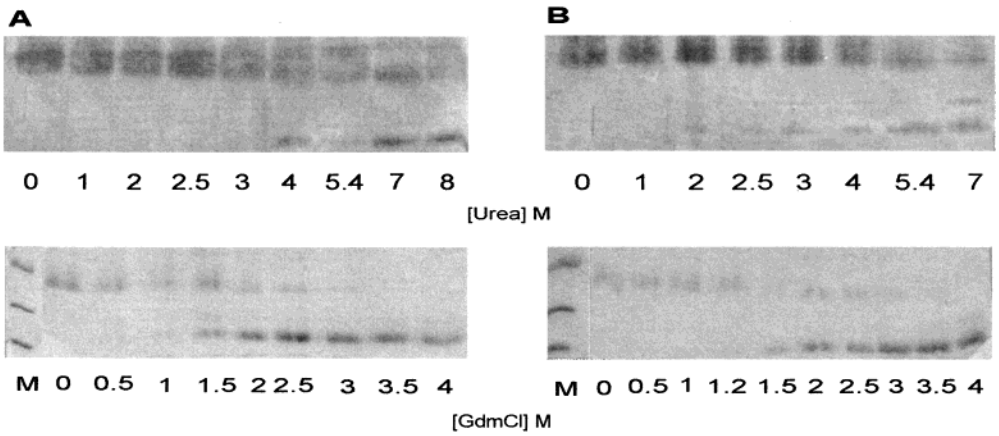

FIGURE 7: SDS−PAGE of glutaraldehyde-cross-linked GSTM1-1 (A) and GSTM2-2 (B) as a function of urea and GdmCl concentrations. Both proteins were incubated for 1 h at 25 °C in the denaturant concentrations shown (pH 6.5) prior to cross-linking.

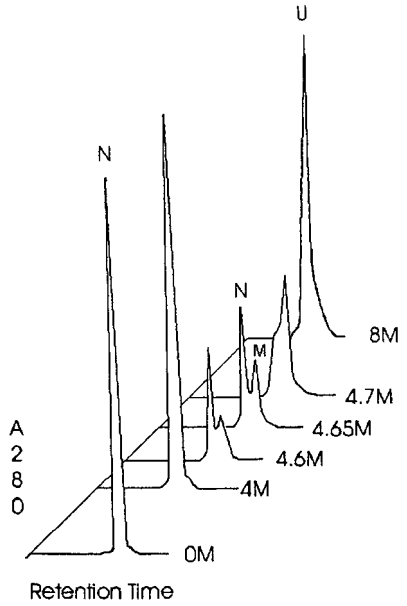

FIGURE 8: SEC−HPLC elution profiles of GSTM2-2 incubated with increasing conentrations of urea. Protein samples (3 μM) were incubated in increasing concentrations of urea for 1 h prior to being injected onto a BioSep SEC−HPLC S3000 column preequilibrated at the same urea concentration. The native protein is labeled (N), folded monomer (M), and unfolded monomer (U).

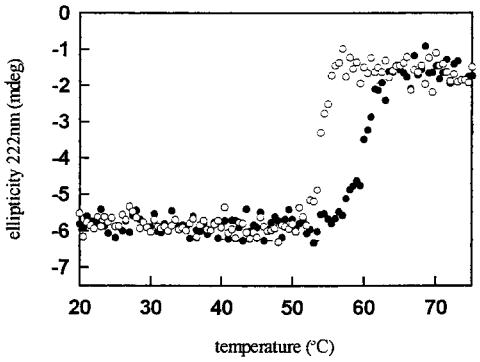

FIGURE 9: Thermal denaturation transition curves of GSTM1-1 (●) and GSTM2-2 (○) measured by circular dichroism at 222 nm.

GSTM1-1 and GSTM2-2, respectively. The sum of the ΔG values (ΔG_1 and ΔG_2) resembles the free energy values obtained for other GST classes, i.e., 21.6 kcal/mol for GSTP1-1 (*19*), 26.8 kcal/mol for GSTA1-1 (*18*), and 26.0 kcal/mol for Sj26GST (*21*), and falls within the range of 20−30 kcal/mol reported for dimeric proteins (*34*). The conclusions drawn from many recent conformational denaturation studies on dimeric proteins have shown that these dimeric proteins may show additional degrees of stability at the quaternary level (*34*). Some examples include λ repressor (*35*), aspartate aminotransferase (*36*), and superoxide dismutase (*37*). A prominent theme raised by these proteins is the benefit of their overall conformations to reduced surface area, increased stability, and novel functions through subunit association.

Although GSTM1-1 and GSTM2-2 are highly homologous proteins (78% identity/94% homology), they display non-

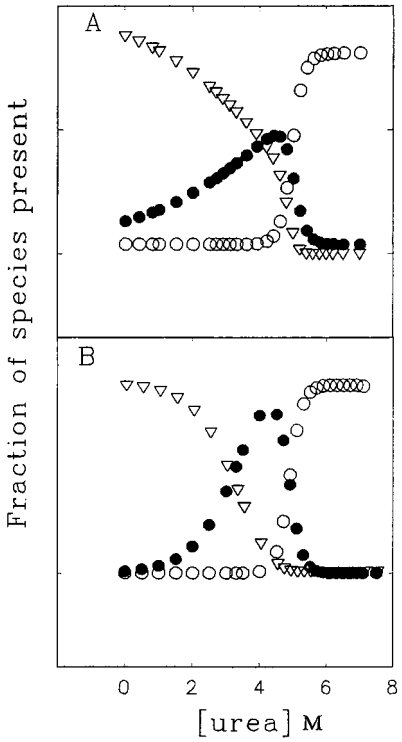

FIGURE 10: Fraction of native (●), intermediate (▽), and unfolded (○) forms of 2 μM GSTM1-1 (A) and GSTM2-2 (B) as a function of urea concentration at pH 6.5, 25 °C, calculated for the tryptophan fluorescence data according to the three-state model $N_2 \leftrightarrow 2I \leftrightarrow 2U$ (see ref *16*).

identical conformational dynamics, the structural basis of which is yet unknown. Their N_2 tertiary structures are not identical as reflected by their different tryptophan environments. Dissociation of the GSTM1-1 dimer to structured monomers occurs at lower denaturant concentrations than those for GSTM2-2. The monomeric intermediate for GSTM1-1 is, however, more stable (i.e., higher ΔG values with urea) than the intermediate for GSTM2-2. The folding intermediates are catalytically inactive and display a native-like secondary structure. The monomeric intermediate formed with GdmCl appears to have a more loosely packed tertiary structure displaying enhanced solvent exposure for its tryptophans and enhanced binding of ANS [these properties have been reported for molten globule-like folding intermediates (*32*)]. An ANS binding monomeric intermediate has been found to be present along the equilibrium unfolding pathway of a class σ GSTS1-1 (*22*).

With respect to class π GST, another group has suggested a three-state equilibrium model based on noncoincident enzyme activity and structural data (*38*). It should be noted that their enzyme assays were performed with denaturant present at the same concentrations used for the structural probes. Because of the dimeric nature of GSTs, a transition from active dimer to inactive unfolded monomer will be protein concentration dependent, thus resulting in the monitored transitions being shifted to lower denaturant concentrations when less protein is used in the assays. A recent study with the yeast dimeric Ure2 protein (*39*) has shown that the dissociation and unfolding of this class θ GST homologue are not closely coupled processes. Stable monomeric intermediates have been observed for GSTs from *Proteus mirabilus* (*40*) and *Bufo bufo* (*41*), whereas stable dimeric and monomeric intermediates have been observed for the squid GSTS1-1 (*22*). The refolding kinetics pathway for class α GSTA1-1 suggests the rapid formation of a monomeric intermediate with nativelike secondary structure (*42*).

In 1991, it was shown with chymotrypsin inhibitor 2 that stable intermediates were not prerequisites for protein folding (*43*). Many other proteins have since been shown to fold successfully without populating any intermediate states. Most proteins greater than 100 residues in length, however, do form populated intermediates when folding. These intermediates vary in conformation and stability; some are nativelike (*44*) while others contain nativelike structure in regions corresponding to a domain of the native protein (*45*). Therefore, the role of intermediate states on the folding pathway needs to be addressed in light of the protein under investigation. Theory suggests that the population of intermediates may slow or increase the rate of protein folding as well as presenting misfolded or dead-end intermediates unable to fold correctly. In some proteins, however, intermediates fold correctly to the native state without undergoing several unfolding steps. The presence of these monomeric intermediates supports a hierarchical folding model (i.e., consecutive folding−association process) in which monomers first fold [perhaps via a multinucleation/condensation process (*46*)] followed by specific recognition of and association with each other and subsequent structural consolidation and reorganization leading to the final tertiary and quaternary structure. In this context, the dimeric structure for class μ GSTs is significant for the formation and stabilization of functional molecules. However, intersubunit interactions do not seem to contribute as significantly toward stabilizing the tertiary structures of the GSTM1 and GSTM2 subunits as reported for members of the class α/π/Sj26 GST group (*18*−*21*) (i.e., class μ subunits appear to be intrinsically more stable). Many homologous proteins with a similar fold also share a similar folding/unfolding mechanism (*47*−*49*), while others show very different folding characteristics (*50, 51*). The molecular origin for the ability of dissociated class μ subunits to exist as stable structured entities at equilibrium is currently under investigation. It might involve interactions peculiar to the GSTM1/M2 subunits and could be topology-related (e.g., the presence of a μ loop in the μ class GSTs, which increases interdomain contacts in each subunit). Protein topology appears to be a major determinant of protein folding (see ref *52*).

ACKNOWLEDGMENT

We thank Osman Bilsel for his invaluable contribution to the data fitting and analysis. H.W.D. thanks the members of the Serrano group for their support during his leave at EMBL.

REFERENCES

1. Milla, M. E., and Sauer, R. T. (1994) *Biochemistry 33*, 1125−1133.
2. Zitzewitz, J. A., Bilsel, O., Luo, J., Jones, B. E., and Matthews, C. R. (1995) *Biochemistry 34*, 12812−15819.
3. Ahmad, N., Srinivas, V. R., Reddy, G. B., and Surolia, A. (1998) *Biochemistry 37*, 16765−16772.
4. Timm, D. E., deHaseth, P. L., and Neet, K. E. (1994) *Biochemistry 33*, 4667−4676.
5. Cheng, X., Gonzalez, M. L., and Lee, J. C. (1993) *Biochemistry 32*, 8130−8139.
6. Mann, C. J., Shao, X., and Matthews, C. R. (1995) *Biochemistry 34*, 14573−14580.
7. Anfinsen, C. B. (1973) *Science 181*, 223−239.
8. Armstrong, R. N. (1997) *Chem. Res. Toxicol. 10*, 2−18.
9. Dirr, H. W., Reinemer, P., and Huber, R. (1994) *Eur. J. Biochem. 196*, 693−698.
10. Holmgren, A. (1995) *Structure 3*, 239−243.
11. Epp, O., Ladenstein, R., and Wendel, A. (1983) *Eur. J. Biochem. 133*, 51−69.
12. Karplus, P. A., Pai, E. F. N., and Schulz, G. E. (1989) *Eur. J. Biochem. 178*, 693−703.
13. Katti, S. K., Robbins, A. H., Yang, Y., and Wells, W. W. (1995) *Protein Sci. 4*, 1988−2005.
14. Wilce, C. J., Board, P. G., Feil, S. C., and Parker, M. W. (1995) *EMBO J. 14*, 2133−2143.
15. Sluis-Cremer, N., Naidoo, N. N., Kaplan, W. H., Manoharan, T. A., Fahl, W. E., and Dirr, H. W. (1996) *Eur. J. Biochem. 241*, 484−488.
16. McTigue, M. A., Williams, D. R., and Tainer, J. A. (1995) *J. Mol. Biol. 246*, 21−27.
17. Ji, X., von Rosenvinge, E. C., Johnson, W. W., Armstrong, R. N., and Gilliland, G. L. (1996) *Proc. Natl. Acad. Sci. U.S.A. 93*, 8208−8213.
18. Wallace, L. A., Sluis-Cremer, N., and Dirr, H. W. (1998) *Biochemistry 37*, 5320−5328.
19. Dirr, H. W., and Reinemer, P. (1991) *Biochem. Biophys. Res. Commun. 180*, 294−300.
20. Erhardt, J., and Dirr, H. W. (1995) *Eur. J. Biochem. 230*, 614−620.
21. Kaplan, W., Husler, P., Klump, H., Erhardt, J., Sluis-Cremer, N., and Dirr, H. (1997) *Protein Sci. 6*, 399−406.
22. Stevens, J. M., Hornby, J. A. T., Armstrong, R. N., and Dirr, H. W. (1998) *Biochemistry 37*, 15534−15541.
23. Zhang, P., Graminski, G. F., and Armstrong, R. N. (1991) *J. Biol. Chem. 266*, 19475−19479.
24. Perkins, S. J. (1986) *Methods Enzymol. 131*, 4−51.

25. Pace, C. N., Shirley, B. A., and Thomson, J. A. (1989) in *Protein Structure, A Practical Approach* (Creighton, T. E., Ed.) pp 311−330, IRL Press, New York.
26. Gloss, L. M., and Matthews, C. R. (1997) *Biochemistry 36*, 5612−5623.
27. Park, Y. C., and Bedouelle, H. (1998) *J. Biol. Chem. 273*, 18052−18059.
28. Park, Y. C., and Bedouelle, H. (1999) *J. Mol. Biol. 286*, 563−577.
29. Lai, Z., McCullock, J., Lashuel, H. A., and Kelly, J. W. (1997) *Biochemistry 36*, 10230−10239.
30. Ji, X., Zhang, P., Armstrong, R. N., and Gilliland, G. L. (1992) *Biochemistry 31*, 10169−10184.
31. Vriend, G. (1990) *J. Mol. Graphics 8*, 52−56.
32. Ptitsyn, O. B., Pain, R. H., Semisotnov, G. V., Zerovnik, E., and Razgulyaev, O. I. (1990) *FEBS Lett. 262*, 20−24.
33. Myers, J. K., Pace, C. N., and Scholtz, J. M. (1995) *Protein Sci. 4*, 2138−2148.
34. Neet, K. E., and Timm, D. E. (1994) *Protein Sci. 3*, 2167−2174.
35. Banik, U., Saha, R., Mandal, N. C., Bhattacharyya, B., and Ray, S. (1992) *Eur. J. Biochem. 206*, 15−21.
36. Leistler, B., Herold, M., and Kirschner, K. (1992) *Eur. J. Biochem. 205*, 603−611.
37. Mei, G., Rosato, N., Silva, N., Jr., Rusch, R., Gratton, E., Savin, I., and Finazzi-Agro, A. (1992) *Biochemistry 31*, 7224−7230.
38. Aceto, A., Caccuri, A. M., Sacchetta, P., Bucciarelli, T., Dragani, B., Rosato, N., Federici, G., and Di Ilio, C. (1992) *Biochem. J. 285*, 241−245.
39. Perrett, S., Freeman, S. J., Butler, P., Jonathan, G., and Fersht, A. R. (1999) *J. Mol. Biol. 290*, 331−345.
40. Sacchetta, P., Aceto, A., Bucciarelli, T., Dragani, B., Santarone, S., Allocati, N., and Di Ilio, C. (1993) *Eur. J. Biochem. 215*, 741−745.
41. Sacchetta, P., Penelli, A., Bucciarelli, T., Cornelio, L., Amicorelli, F., Miranda, M., and Di Ilio, C. (1999) *Arch. Biochem. Biophys. 369*, 100−106.
42. Wallace, L., and Dirr, H. W. (2000) *Biochemistry* (in press).
43. Jackson, S. E., and Fersht, A. R. (1991) *Biochemistry 30*, 10428−10435.
44. Lorch, M., Mason, J. M., Clarke, A. R., and Parker, M. J. (1999) *Biochemistry 38*, 1377−1385.
45. Cavagnero, S., Dyson, H. J., and Wright, P. E. (1999) *J. Mol. Biol. 285*, 269−282.
46. Fersht, A. R. (1995) *Proc. Natl. Acad. Sci. U.S.A. 92*, 10869−10873.
47. Lang, K., Krebs, H., Schmid, F. X., and Bientema, J. J. (1986) *FEBS Lett. 204*, 135−139.
48. Hooke, S. D., Radford, S. E., and Dobson, C. M. (1994) *Biochemistry 33*, 5867−5876.
49. Saddei, N., Chiti, F., Paoli, P., Fiaschi, T., Bucciantini, M., Stefani, M., Dobson, C. M., and Ramponi, G. (1999) *Biochemistry 38*, 2135−2142.
50. Plaxco, K. W., Spitzfaden, C., Campbell, I. D., and Dobson, C. M. (1997) *J. Mol. Biol. 270*, 763−770.
51. Burns, L. L., Dalessio, P. M., and Ropson, I. J. (1998) *Proteins: Struct., Funct., Genet. 33*, 107−118.
52. Martinez, J. C., and Serrano, L. (1999) *Nat. Struct. Biol. 6*, 1010−1016.

BI000176D